Korean J. Chem. Eng., 32(2), 274-283 (2015)
DOI: 10.1007/s11814-014-0216-y

pISSN: 0256-1115
eISSN: 1975-7220

Kinetics and equilibrium studies on removal of methylene blue and methyl orange by adsorption onto activated carbon prepared from date pits-A comparative study

Khaled Mahmoudi†, Khaled Hosni, Noureddine Hamdi, and Ezzeddine Srasra

Laboratory of Physicochemical of Minerals Materials and its Applications,
National Centre of Research in Materials Sciences (CNRSM), B.P.73-8020, Soliman, Tunisia
(*Received 16 February 2014 • accepted 30 July 2014*)

Abstract−The adsorption of Methylene blue and Methyl orange by date pits carbon was carried out by varying parameters such as agitation time, pH and dye concentration. Equilibrium adsorption data followed both Langmuir and Freundlich isotherms. Adsorption followed second-order rate kinetics. The adsorption capacity was found to be 434 and 455 mg of methyl orange and methylene blue, respectively, per g of the date pits carbon. Acidic pH is favorable for the adsorption of methyl orange against a basic medium which is favorable for the adsorption of MB. An opposite result was found for the methylene blue adsorption.

Keywords: Activated Carbon, Adsorption, Methylene Blue, Methyl Orange

INTRODUCTION

Environmental contamination is a major problem being faced by society today. Industrial, agricultural and domestic wastes, due to the rapid development in the technology, are discharged in the several receivers. Generally, this discharge is directed to the nearest water sources such as rivers, lakes and seas. While the rates of development and waste production are not likely to diminish, efforts to control and dispose of wastes are appropriately rising.

Wastewaters from textile industries represent a serious problem all over the world. They contain different types of synthetic dyes which are known to be a major source of environmental pollution in terms of both the volume of dye discharged and the effluent composition [1]. For the volume of wastewater containing processed textile dyes it is annually estimated that 1-15% of the dye is lost in the effluents during the dyeing process [2] steady increase. Among 7×105 tones and approximately 10.000 different types of dyes and pigments are produced worldwide. Most of these dyes are toxic, mutagenic and carcinogenic. Moreover, they are very stable to light, temperature and microbial attack, making them recalcitrant compounds. From an environmental point of view, the removal of synthetic dyes is of great concern.

Many studies have been conducted on the toxicity of dyes and their impact on the ecosystem [3], as well as the environmental issues associated with the manufacture and subsequent usage of dyes [4]. Biological treatment processes are reported to be efficient in the removal of suspended solids and reduction of chemical oxygen demand but are largely ineffective in removing color from waste water [5]. Hence, investigations have been conducted on physico-chemical methods of removing color from textile effluent. These +-filtration [8], electro-chemical [9] and adsorption [5] techniques. The advantages and disadvantages of each technique have been extensively reviewed [10]. Of these, adsorption has been found to be an efficient and economic process to remove dyes, pigments and other colorants and also to control the bio-chemical oxygen demand [5,11].

Activated carbon (AC), inorganic oxides, natural adsorbents (such as clays and clay minerals, cellulosic materials, chitin and chitosan) have been extensively used as adsorbents [12-18].

Activated carbons (AC) are the most versatile and commonly used adsorbents because of their extremely high surface areas, micropore volumes [19] large adsorption capacities, fast adsorption kinetics, and relative ease of regeneration [20].

Despite its prolific use in water and waste water industries, commercial activated carbon (CAC) remains an expensive material. This has led to a search for low-cost materials as alternative adsorbent materials [14]. In contemporary research, different agricultural biomass-based raw materials like olive stones [21], date pits [22,23], rice husk [24], and jute stick [25] have been investigated in the last years as activated carbon.

The purpose of this work was to study the kinetics and the mechanism of adsorption of methylene blue (MB), and methyl orange (MO) onto date pits activated carbon, prepared by chemical activation using $ZnCl_2$ as an activating agent, and to compare the adsorption for the removal of the cationic and anionic dyes under optimum experimental conditions. Thus, this investigation is studying the adsorption parameters (pH, time and dye concentration) of adsorption of MB and MO on date pits before and after activation.

EXPERIMENTAL

1. Materials and Methods

1-1. Material Preparation

Date pits constitute approximately 10% of the total weight of dates [26], making them the largest agricultural by-product in palm growing countries, including Tunisia. Raw material (date pits) used for

†To whom correspondence should be addressed.
E-mail: mahmoudikhaled1984@gmail.com

preparation of activated carbon was procured locally, washed, dried at 423 K, crushed to desired mesh size (0.5-1.0 mm). This material was impregnated with concentrated solution of $ZnCl_2$, using impregnation ratios $ZnCl_2$/date pits of 2 : 1 (w/w) followed by heating, under nitrogen atmosphere, for 2 hours, in a modified electric furnace at 400 °C with constant heating of 10°/min. The activated product was then cooled to room temperature and washed several times with hot deionized water until the pH of the washing solution reached 6-7. The final product was dried in an oven at 105 °C for 24 h.

1-2. Characterization of Materials

Textural characterization of the activated carbon (AC) was carried out by N_2 adsorption at 77 K using Autosorb I, supplied by Quantachrome Corporation, USA. The BET (N_2, 77 K) is the most usual standard procedure used when characterizing an activated carbon [27]. The morphology of raw material and activated carbons produced from date pits were examined using scanning electron microscopy (Philips Fei Quanta 200).

Surface functional groups were detected by Fourier transform infrared (FT-IR) spectroscopy to identify the functional groups at the surface of carbon materials. The infrared spectra were recorded as KBr pellets using a Perkin-Elmer FT-IR (model 783) instrument. KBr pellets were prepared by mixing 5 wt% of absorbent with 95 wt% KBr and pressing.

Acidic functional groups were determined by Boehm's method of titration with basic solutions of different base strengths ($NaHCO_3$, Na_2CO_3, NaOH, C_2H_5ONa) [32,33]. This was achieved by accurately weighing 1.00 g sample into four conical flasks with stopper. Samples were agitated for 16 h with 0.05 N solutions of different base strengths. The amount of Na^+ ions remaining in the solution was determined by adding an excess of standard HCl and back-titration method. The basic groups' contents of the oxidized samples was determined with 0.05 N HCl [33,34].

The point of zero charge (*PZC*) was determined using the batch equilibrium method which proposed by Milongic et al. [31]. Accordingly, the samples of AC (0.15 g) were shaken in PVC vials, for 48 h, with 50 ml of 0.01 M KCl, at different pH values. Initial pH values were obtained by adding a certain amount of KOH or HCl solution so as to keep the ionic strength constant. Experimental results of the pH_{PZC} determination are presented as pH values of filtered solutions equilibration (pH_{final}) with the adsorbent as a function of initial pH value ($pH_{initial}$). It can be seen that PZC is at pH=5.9 and 4.01 (pH_{final} level, where common plateau is obtained) for raw date pits and activated carbon, respectively.

1-3. Adsorption Study

All solutions were prepared and stocked in polyethylene flasks. All sorption experiments were performed in 50 ml polyethylene tubes. Stock solutions of MB and MO (1,000 mg·l^{-1}) were prepared and suitably diluted to the required initial concentrations. Adsorption experiments were at room temperature (around 25 °C) under batch mode [32].

The time-dependent sorption of dye on raw date pits and activated carbon was carried out with 100 mg of the adsorbent and 50 ml of 1,000 mg·l^{-1} dye solution. The mixtures were stirred at low speed (~100 rpm) for different time intervals (0.5-24 h). After separating the turbidity by centrifugation and through the standard filter designed for a wide range of laboratory applications. The final concentration of dye (C_f) of MB or MO was obtained by measuring O.D. at 663 nm and 465 nm, at pH=7 (λ_{max}) for MB and MO, respectively, using a Perkin Elmer UV-visible spectrophotometer (Model:680).

The pH-dependent experiments were carried out by adjusting the initial pH (in the 2-12 range) of the dye solution (1,000 mg·l^{-1}) using 0.1 M HCl or 0.1 M NaOH solutions. 100 mg of raw date pits or activated carbon was weighed in polyethylene tubes and 25 ml of the stock solution with adjusted pH was added and stirred for 6 h. Then, the pH was measured again; the mixtures were centrifuged and supernatant dye concentrations were determined.

The adsorption isotherms were obtained by batch equilibrium technique. One hundred milligrams of raw date pits or activated carbon was weighed in polyethylene tubes and then these were filled with 25 ml of aqueous solutions of MO (pH~3.5) or MB (pH~9) ranging in concentration from 0 to 1,000 mg·l^{-1}. The mixtures were stirred for 4 h at room temperature, centrifuged and the supernatant dye concentrations were determined.

The samples were filtered prior to analysis to minimize interference of the carbon fines with the analysis. Each experiment was duplicated under identical conditions. Blanks containing no dye were used for each series of experiments as controls. The amount of adsorption at equilibrium, q_e (mg g^{-1}), was calculated by:

$$q_e = \frac{(C_0 - C_e) \times V}{w}$$

where C_0 and C_e (mg·l^{-1}) are the liquid-phase concentrations of dye at initial and equilibrium, respectively. V is the volume of the solution and w is the mass of dry adsorbent used (g).

1-4. Desorption Experiments

For the desorption study, 0.05 g of activated carbon was added to 25 cm^3 of dye solution (1,000 mg/L) and the mixture was stirred at 4 hours. After mixing, the supernatant dyes solution was discarded and the activated carbon alone was separated. The activated carbon was washed gently with distilled water to remove the dye present on its surface (unadsorbed dye). Then, the dye-adsorbed activated carbon was added into 25 cm^3 of distilled water. Distilled water and activated carbon (saturated with dye) solution samples were taken at specific time intervals (5, 10, 20, 30, 60…. 240 min).

The amount of dye desorbed from activated carbon, qt (mg/g), was calculated at different values of time (5 to 240 min) by the relationship above.

RESULTS AND DISCUSSION

1. Characteristics of the Adsorbents

1-1. Textural and Surface Characterization

Fig. 1(a) shows the N_2 adsorption-desorption isotherms of the raw date pits and the activated carbons prepared at the carbonization temperatures of 400 °C, where V_{ads} and P/P_0 are the amount of N_2 adsorbed and relative pressure, respectively. According to the IUPAC classification, these isotherms feature an intermediate between types I and II [27]. Interestingly, a slight hysteresis was observed in the isotherm, which suggests the existence of mesopores in the activated carbon, and as shown in N_2 adsorption-desorp-

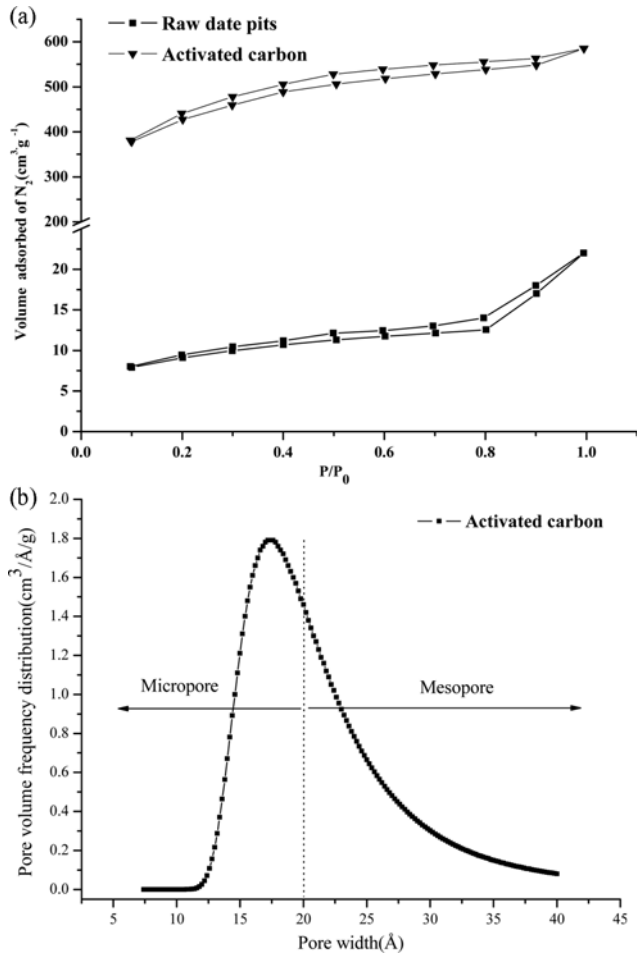

Fig. 1. (a) Adsorption/desorption isotherms of N_2 for raw date pits and activated carbon. (b) Pore size distribution of activated carbon.

tion isotherm of Fig. 1(a), the CA has a high adsorption uptake at low relative pressure (P/P_0), indicative of the existence of micropores. The pore size distribution curve obtained using D-A method, which is displayed in Fig. 1(b), shows two regions: (1) micropores (<20 Å); (2) mesopores (>20 Å).

As shown in Table 1, a BET calculation gives the BET surface area for the activated carbon equal to 1,380 m^2/g, much greater than the 25 $m^2 \cdot g^{-1}$ value obtained for its precursor (Raw date pits); and the t-plot method gives the surface areas of micropores and external large-sized pores equal to 1,100 and 280 m^2/g, respectively. Moreover, the total pore volume is calculated to be 0.91 cm^3/g according to the amount adsorbed at a relative pressure P/P_0 of 0.99 and the V_{micro} value of activated carbon was reported to be 0.49 $cm^3 \cdot g^{-1}$ more than 0.3 $cm^3 \cdot g^{-1}$ reported in the literature [33].

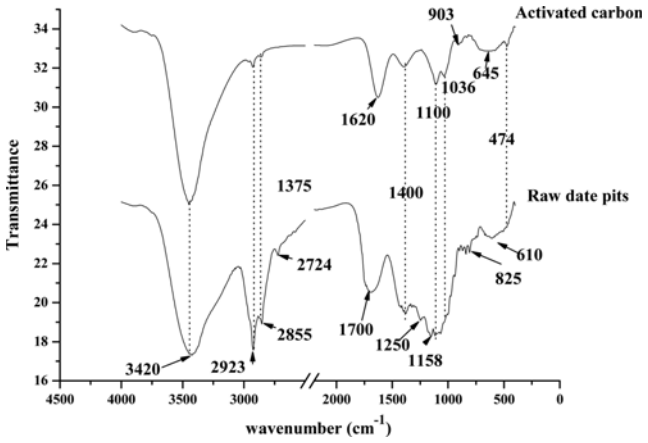

Fig. 2. FTIR of the date pits before and after activation.

1-2. Functional Groups

Fig. 2 shows the FT-IR spectra for the activated carbon and the raw date pits. The FTIR spectra of the raw date pits and the AC show strong broad overlapping band located at 3,420 cm^{-1} which is ascribed to O-H stretching vibration in hydroxyl groups of glucose [34]. Two bands observed at 2,923 and 2,855 cm^{-1} are assigned to asymmetric C-H and symmetric C-H bands, respectively, present in alkyl groups such as methyl and methylene groups [34]. Stretching absorption band at 1,700 cm^{-1} is assigned to carbonyl C=O present in esters, aldehydes, ketone and carboxyl groups [35]. The bands at 1,250 and 825 cm^{-1} may be connected with esters such as CH_3-CO-O- as well as with cyclic C-O-C groups conjugated with carbon-carbon doubles C=C-O-C in olefinic or aromatic structures which represent the major components in the lignocellulosic material, e.g. -O-CH_3 in ethers [36]. The band at 1,158 cm^{-1} was assigned to presence of cellulose C-O-C [41]. One later band at 610 cm^{-1} is ascribed to υ O-H in OH groups, this low region than the expected where it seems non-free and involved in hydrogen bonds [38,39]. The presence of the bands between 903 and 825 cm^{-1} in raw date pits spectra is attributed to the vibration of aromatic substitution [41].

The surface chemistry of activated carbons essentially depends on their heteroatom content, mainly on their surface oxygen complex content. They determine the charge of the surface, its hydrophobicity, and the electronic density of the graphene layers. Fig. 3 shows that activated carbon from date pits showed amphoteric behavior, with a surface acidity of 5.9 mmol/g and a surface basicity 0.72 mmol/g. When a solid such as a carbon material is immersed in an aqueous solution, it develops a surface charge that comes from the dissociation of surface groups or the adsorption of ions from solution [41]. This surface charge will depend on the solution pH and the surface characteristics of the carbon. A negative charge results

Table 1. Physical and chemical characteristics of the adsorbent

Adsorbent	S_{BET} (m^2g^{-1})	S_{micro} (m^2g^{-1})	V_t (cm^3g^{-1})	$V\mu$ (cm^3g^{-1})	pH_{PZC}	Acidity (mmol/g)	Basicity (mmol/g)
Raw date pits	25	--	0.07	0	5.9	2.5	1.82
Activated carbon	1380	1100	0.91	0.49	4.01	5.9	0.72

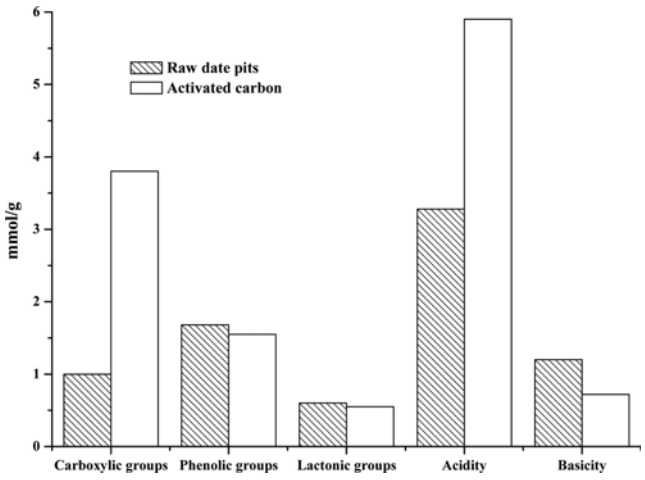

Fig. 3. Histogram summarizing the surface acidity of natural date pits before and after activation.

from the dissociation of surface oxygen complexes of acid character such as carboxyl and phenolic groups (carboxylic, anhydrides, lactones and phenols) [42]. Therefore, these surface acid sites are of Brønsted type. The origin of the positive surface charge is more uncertain, but it can be due to surface oxygen complexes of basic character like pyrones or chromenes [43] or to the existence of electron-rich regions within the graphene layers acting as Lewis basic centers, which accept protons from the aqueous solution.

1-3. Scanning Electron Microscopy

Fig. 4(a) and Fig. 4(b) show that the surface of natural date pits was quite dense without any pores except for some occasional cracks. This would account for its poor or negligible BET surface area. In the micrograph of the activated carbon prepared at 400 °C (Fig. 4(c) and 4(d)), a small pores, transitional pores and large pores with different shapes were clearly identified, which account for the higher BET surface area and micropore volume.

2. Adsorption Process of MO and MB Molecules on Activated Carbon: Equilibrium

2-1. Effect of pH on MO and MB Adsorption

The effect of solution pH on dye removal from solution was studied under identical conditions for the two dyes chosen for this study. The data are presented in Fig. 5, which indicate that the adsorption behavior of each of the reactive dyes was different, from pH 2

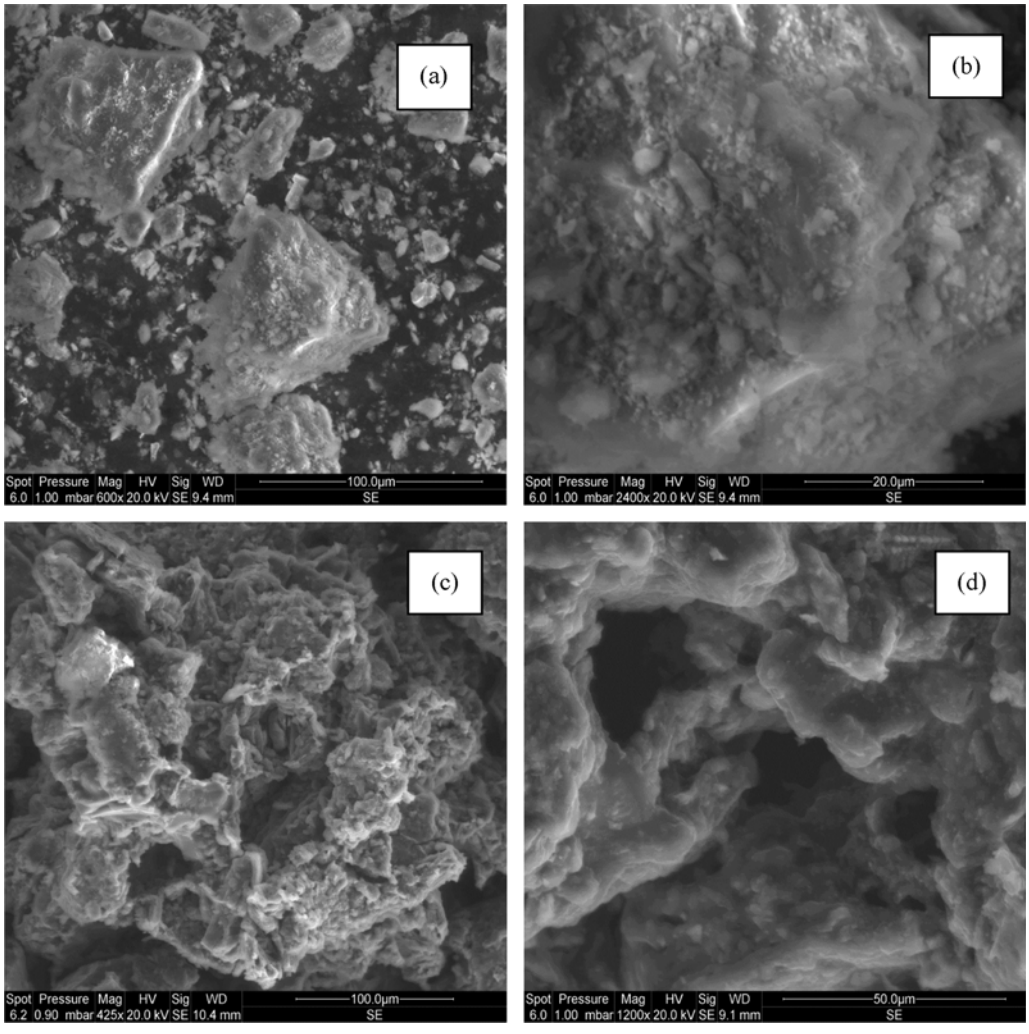

Fig. 4. SEM of activated carbon from natural pits (a), (b) and date pits at 400 °C (c), (d).

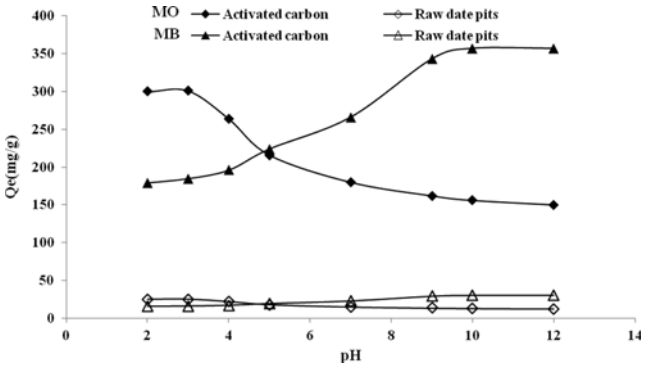

Fig. 5. Effect of pH on the adsorption of methylene blue and methyl orange onto date pits activated carbon (Temperature 25 °C, contact time=300 min, initial dyes concentrations=1,000 mg/*l*, DPAC dosage=0.1 g/50 ml (dyes).

to pH 12. The removal of methyl orange decreased, when the pH was increased from 2 to 12, with the percentage removal then remaining almost constant up to pH=8). A large decrease in adsorption capacity for this dye was observed under basic conditions. Similar adsorption behavior with variation in solution pH has been reported in the literature [44]. The removal of the methylene blue increased, with the increasing of the pH.

The adsorption mechanism for the dyes adsorption is electrostatic interaction; the removal capacity of the MO is at a maximum within the range pH 2-4. In this pH range the surface of activated carbon was positively charged (pH_{pzc}=4.1) and MO was negatively charged (pKa of dye 4.4-5.5). The protonated groups of activated carbon are mainly carboxylic group ($-CO-OH_2^+$), phenolic ($-OH_2^+$). The deprotonated groups of the methyl orange dye were probably the sulfonate groups ($-SO_3^-$). At solution pH≤4, the removal capacity of MO was expected to decrease, as the adsorbent was positively charged and dye molecules were either neutral or partially positively charged. At this acidic pH, the sulfonate groups of the dyes were almost protonated ($-SO_3H$, i.e., neutral). Furthermore, the protonation of nitrogen atoms especially those not involved in aromatic systems, is also probable. The large reduction in dye adsorption at highly basic conditions can be attributed to electrostatic repulsion between the negatively charged activated carbon and the deprotonated dye molecules. For the methylene blue (MB) the removal capacity of the dye is at a maximum at basic medium. In this pH range the surface of activated carbon is negatively charged and MB was positively charged ($-S^+$). The deprotonated groups of activated carbon are mainly carboxylic group ($-CO-O^-$), phenolic ($-O^-$). At solution pH≥4, the removal capacity of MB was expected to increase, as the adsorbent was negatively charged and dye molecules were positively charged. The constant adsorption capacity of activated carbon for dyes over the pH≥9 was an indication that the electrostatic mechanism was not the only mechanism for dye adsorption in this system. Activated carbon can also interact with dye molecules via hydrogen bonding and hydrophobic-hydrophobic mechanisms [44].

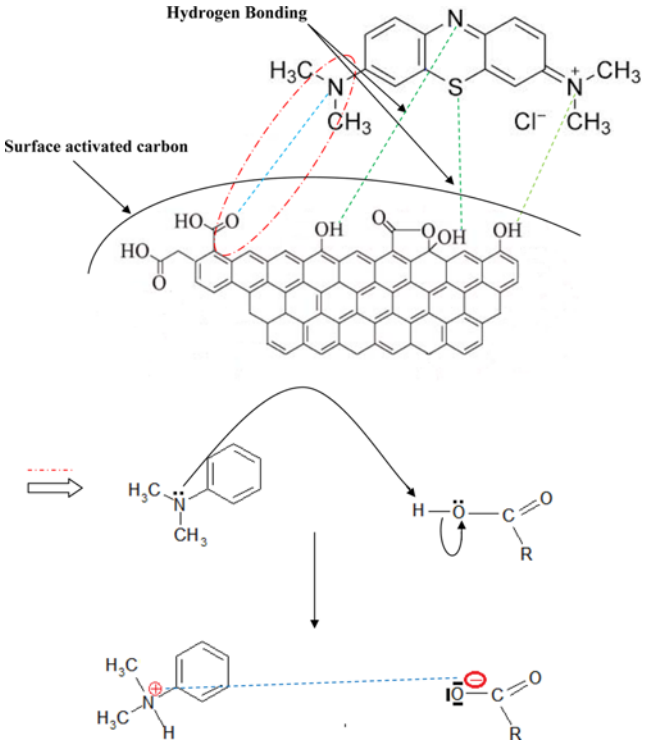

Fig. 6. Mechanism of adsorption.

The probable mechanism of adsorption is given in Fig. 6.

2-2. Effect of Agitation Time on Adsorption Dyes

The effect of contact time on the amount of dyes adsorbed was investigated at the optimum initial concentration of dye, and the data are presented in Table 2. As can be seen from Fig. 7 the extent of removal (in terms of q_e) of MB and MO by activated carbon and raw date pits was found to increase with time, at some point in time, reach a maximum value beyond which no more was removed from solution. At this point, the amount of the dye desorbing from the adsorbent is in a state of dynamic equilibrium with the amount of the dye being adsorbed onto the adsorbent. The time required to attain this state of equilibrium is termed the equilibrium time, and the amount of dye adsorbed at the equilibrium

Table 2. Kinetic parameters for the adsorption of MB and MO onto natural date pits before and after activation at 25 °C

Samples	Dye	$q_{e:exp}$ ($mg \cdot g^{-1}$)	First-order kinetic model				Second-order kinetic model			
			k_1 ($l\ g^{-1} \cdot h^{-1}$)	$q_{e:calc}$ ($mg \cdot g^{-1}$)	R^2	Δq %	k_2 ($g \cdot h^{-1} \cdot mg^{-1}$)	$q_{e:calc}$ ($mg \cdot g^{-1}$)	R^2	Δq %
Raw date pits	MB	45	0.49	2.6	0.51	94.22	0.142	45.5	0.999	1.11
	MO	27	0.373	1.26	0.52	95.33	0.386	27.17	0.999	0.62
Activated carbon	MB	403	0.748	200.5	0.993	50.24	0.003	416.5	0.999	3.34
	MO	301	0.739	73	0.87	78.74	0.006	312.5	0.999	3.82

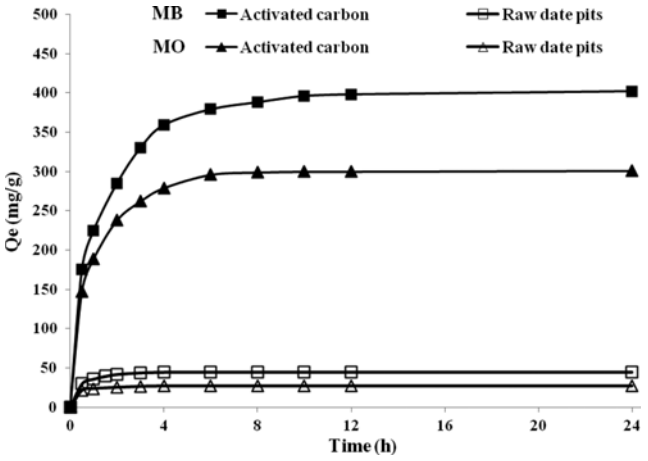

Fig. 7. Effect of time for the adsorption of methylene blue and methyl orange on date pits before and after activation.

time reflects the maximum adsorption capacity of the adsorbent under those operating conditions. The contact time necessary for MB and MO dyes with initial concentrations of 500 mg l^{-1} to reach equilibrium is 1 h for raw date pits. However, both for MB and MO dyes with initial concentrations (500 mg l^{-1}), longer equilibrium time of 10 h are needed using activated carbon as absorbent.

The adsorption capacity at equilibrium increases from 45 and 27 mg·g^{-1}, respectively for MB and MO for the raw date pits as adsorbent to 300 and 400 mg·g^{-1} for the activated carbon as adsorbent. It is evident that the activated carbon prepared from date pits is efficient to adsorb MB and MO dyes from aqueous solution, the process attaining equilibrium gradually. This is because activated carbon is composed of porous structure with large internal surface area (1,380 $m^2 \cdot g^{-1}$).

In batch type adsorption systems, a monolayer of adsorbate is normally formed on the surface of adsorbent [45] and the rate of removal of adsorbate species from aqueous solution is controlled primarily by the rate of transport of the adsorbate species form the exterior/outer sites to the interior sites of the adsorbent particles [46,47].

Kinetic modeling not only allows estimation of sorption rates but also leads to suitable rate expressions characteristic of possible reaction mechanisms. In this respect, two kinetics, the pseudo-first-order (Eq. (1)) and pseudo-second-order equation (Eq. (2)) [48], were tested.

The pseudo first-order equation is given by Lagergren and Svenska [19]:

$$\ln(q_e - q_t) = \ln q_e - k_1 t \quad (1)$$

where q_e and q_t are the amounts of MB or MO adsorbed (mg·g^{-1}) at equilibrium and at time t (min), respectively, and k_1 the rate constant adsorption (h^{-1}). Values of k_1 were calculated from the plots of $\ln(q_e - q_t)$ versus t (Fig. 8). Although the correlation coefficient values are higher than 0.51 for activated carbon, the experimental q_e values do not agree with the calculated ones, obtained from the linear plots (Table 2). This shows that the adsorption of MB and MO onto activated carbon and raw date pits is not a first-order kinetic.

On the other hand, a pseudo second-order equation based on equilibrium adsorption [54] is expressed as:

$$\frac{1}{q_t} = \frac{1}{k_2 q_e^2} + \frac{t}{q_t} \quad (2)$$

where k_2 (g/mg·h^{-1}) is the rate constant of second-order adsorption. If second-order kinetics is applicable, the plot of t/q versus t should show a linear relationship. There is no need to know any parameter beforehand and q_e and k_2 can be determined from the slope and intercept of the plot. Also, this procedure is more likely to predict the behavior over the whole range of adsorption. The linear plots of t/q versus t (Fig. 9) show a good agreement between experimental and calculated adsorption capacity values Δq (%) (Table 2). The correlation coefficients for the second-order kinetic model are greater than 0.99, indicating the applicability of this kinetic equation and the second-order nature of the adsorption process of MB and MO on activated carbon and raw date pits.

It is found (Table 2) that the adsorption of methylene blue and methyl orange on activated carbon and raw date pits can be best described by the second-order kinetic model. Similar phenomenon processes have been observed in the adsorption of direct dyes on activated carbon prepared from sawdust [51] and adsorption of Congo red dye on activated carbon from coir pith [52].

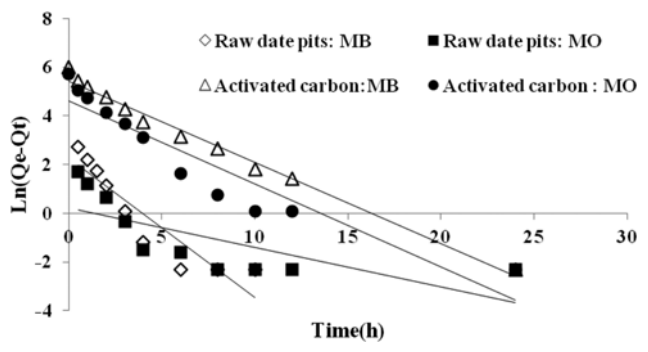

Fig. 8. Pseudo-first order kinetic plot for the adsorption of methyl orange and methylene blue on natural date pits before and after activation.

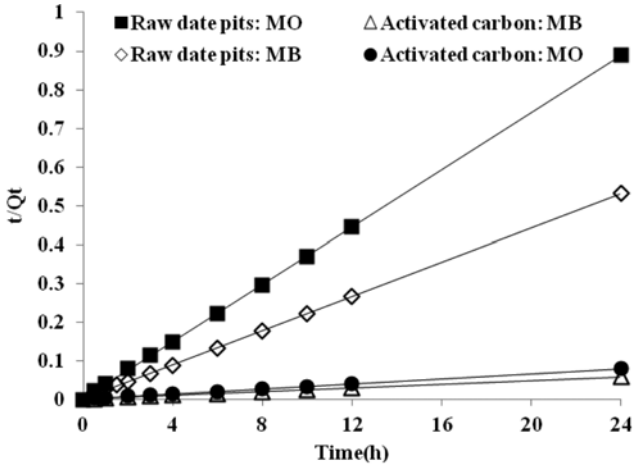

Fig. 9. Pseudo-second order kinetic plot for the adsorption of MO and MB on natural date pits before and after activation.

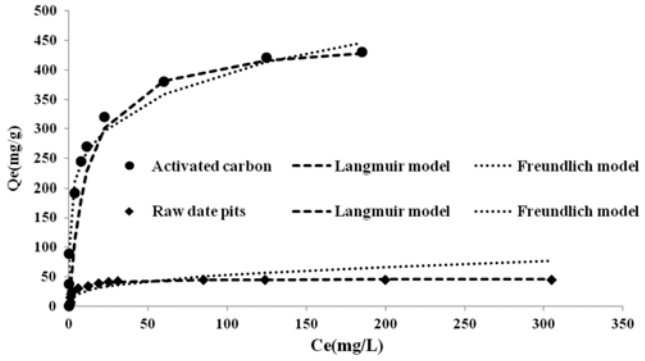

Fig. 10. Equilibrium isotherms for methyl orange on date pits before and after activation.

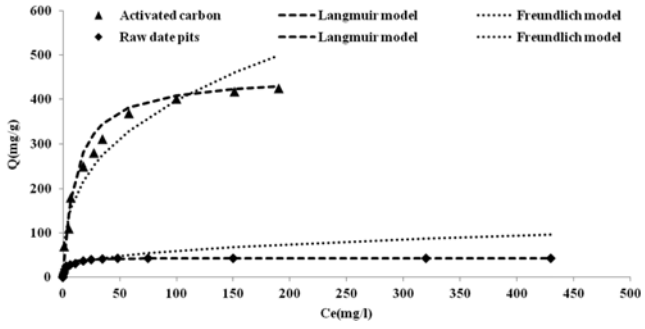

Fig. 11. Equilibrium isotherms for methylene blue on date pits before and after activation.

2-3. Adsorption Isotherms

The adsorption isotherm indicates how the adsorption molecules distribute between the liquid phase and the solid phase when the adsorption process reaches an equilibrium state. The analysis of the isotherm data by fitting them to different isotherm models is an important step to find the suitable model that can be used for design purpose [53].

Fig. 10 and Fig. 11 typically show the adsorption isotherms of MB and MO dyes at 25 °C on the activated carbon and her precursor (date pits). Adsorption isotherm is basically important to describe how dyes interact with adsorbents, and is critical in optimizing the use of adsorbents.

Adsorption isotherm study is carried out on two well-known isotherms, Langmuir and Freundlich. The Langmuir isotherm assumes monolayer adsorption onto a surface containing a finite number of adsorption sites of uniform strategies of adsorption with no transmigration of adsorbate in the plane of surface [45]. Whereas, the Freundlich isotherm model assumes heterogeneous surface energies, in which the energy term in the Langmuir equation varies as a function of the surface coverage [45]. The applicability of the isotherm equation is compared by judging the correlation coefficients, R^2.

Langmuir isotherm

The linear form of Langmuir's isotherm model is given by the following equation:

$$\frac{C_e}{q_e} = \frac{1}{Q_0 b} + \left(\frac{1}{Q_0}\right) C_0$$

where C_e is the equilibrium concentration of the adsorbate (MB/MO) (mg/*l*), q_e the amount of adsorbate adsorbed per unit mass of adsorbate ($mg \cdot g^{-1}$), and Q_0 and b are Langmuir constants related to adsorption capacity and rate of adsorption, respectively. When C_e/q_e was plotted against C_e, straight line with slope $1/Q_0$ was obtained, indicating that the adsorption of MB on activated carbon follows the Langmuir isotherm. The Langmuir constants 'b' and 'Q_0' were calculated from this isotherm and their values are given in Table 3.

Conformation of the experimental data into the Langmuir isotherm model indicates the homogeneous nature of raw date pits and activated carbon surfaces, i.e., each dye molecule/adsorbent adsorption has equal adsorption activation energy. The results also demonstrate the formation of monolayer coverage of dye molecule at the outer surface of raw date pits and activated carbon. Similar observation was reported by the adsorption of acid orange 10 dye onto activated carbons prepared from agricultural waste bagasse [54] and by the adsorption of direct dyes on activated carbon prepared from sawdust [51] and adsorption of Congo red dye on activated carbon from coir pith [52].

The essential characteristics of the Langmuir isotherm can be expressed in terms of a dimensionless equilibrium parameter (R_L) [58], which is defined by:

$$R_L = \frac{1}{1 + bC_0}$$

where b is the Langmuir constant and C_0 the highest dye concentration ($mg \cdot l^{-1}$). The value of R_L indicates the type of the isotherm to be either unfavorable ($R_L>1$), linear ($R_L=1$), favorable ($0<R_L<1$) or irreversible ($R_L=0$). Values of RL ranged between 0.002 and 0.01 ($0<R_L<1$). These values c onfirm that the raw date pits and activated carbon are favorable for adsorption of MB and MO dye under conditions used in this study.

Table 3. Isotherms parameters obtained by Langmuir and Freundlich models for removal of MB and MO by activated carbon and raw date pits

Adsorbent		Constants Langmuir				Constants Freundlich		
		b (L/mg)	Q_e (mg/g)	R_L	R^2	1/n	K_F	R^2
Raw date pits	MO	0.267	46	0.010	0.99	0.32	11.76	0.94
	MB	0.73	42.5	0.002	0.99	0.25	12.4	0.92
Activated carbon	MO	0.092	434	0.017	0.99	0.39	60.5	0.90
	BM	0.203	455	0.009	0.99	0.36	110	0.91

Table 4. Comparison of maximum adsorption capacity (Q_m) of MB and MO onto activated carbons

Adsorbent	Dye	Q_m (mg·g^{-1})	Reference
Activated carbon from *Phragmites australis*	MO	238.10	[59]
Multiwalled carbon nanotubes	MO	52.86	[60]
Activated carbon from lignin	MO	300	[61]
Chitosan	MO	34.83	[62]
Layered double hydroxides	MO	285	[63]
Activated carbon from date pits at 400 °C	MO	434	This study
Activated carbon from wood	MB	200	[64]
Activated carbon from coffee waste	MB	188.7	[65]
Activated carbon from apricot stones	MB	221.3	[66]
Activated carbon from date pits at 400 °C	MB	455	This study
Activated carbon from date pits	MB	244	[22]
	Remazol dyes	173	

Freundlich isotherm

The well-known logarithmic form of the Freundlich model is given by the following equation:

$$\log q_e = \log K_F + \left(\frac{1}{n}\right)\log C_e$$

where q_e is the amount adsorbed at equilibrium (mg·g^{-1}), C_e the equilibrium concentration of the adsorbate and K_F and n are Freundlich constants, n giving an indication of how favorable the adsorption process, and K_F is the adsorption capacity of the adsorbent. K_F can be defined as the adsorption or distribution coefficient and represents the quantity of dye adsorbed onto activated carbon adsorbent for a unit equilibrium concentration. The slope 1/n ranging between 0 and 1 is a measure of adsorption intensity or surface heterogeneity, becoming more heterogeneous as its value gets closer to zero [56]. A value for 1/n below unity indicates a normal Langmuir isotherm, while 1/n above unity is indicative of cooperative adsorption [57]. The plot of $\log q_e$ versus $\log C_e$ gives straight lines with slope '1/n'). The Freundlich constants (K_F and n) were calculated and recorded in Table 3.

A comparison is made between the isotherms plotted in Fig. 10 and Fig. 11, which show the experimental data points and the theoretical isotherms plotted on the same graph. As seen from Table 3, the Langmuir model yields a somewhat better fit both for MB and MO, for raw date and the activated carbon, than the Freundlich model. As also illustrated in Table 3, the value of 1/n is ranging between 0 and 1 for MB and MO, which indicates favorable adsorption [58]. Table 3 lists the comparison of maximum monolayer adsorption capacity of MB and MO dyes on raw date pits and date pits activated carbon.

The data shows that the activated carbon studied in this work has very large adsorption capacity. The value of the maximum adsorption capacities, Qo=455 and 434 mg·g^{-1} for MB and Mo, respectively. The removal of dye by different adsorbents has been studied in recent years and some of these reports provide Q values. Although these values were obtained under different ranges of conditions, they can be a useful criterion of the adsorbent capacity. The Q value obtained in this study is greater than those of reported for Chitosan (34.83 mg/g for MO) [62], Activated Carbon from *Phragmites australis* (238.10 mg/g for MO) [59], layered double hydroxides (285 mg/g for MO) [63], Activated carbon from date pits (244 mg/g for MB) [67] and activated carbon from lignin (300 mg/g for MO) [61] (Table 4).

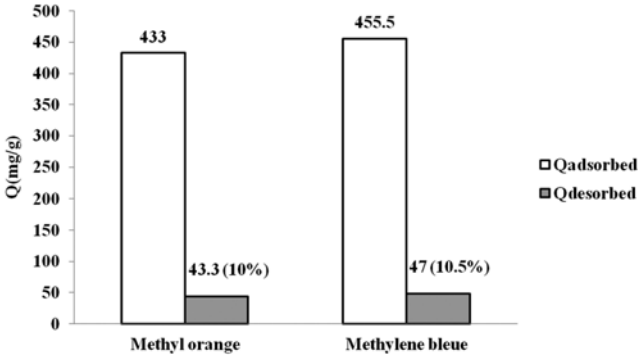

Fig. 12. Comparison between the amount adsorbed and desorbed.

Fig. 12 shows the comparison between the amount adsorbed and desorbed for methylene blue and methyl orange. According to the desorption study, we noted for the two types of dyes (methylene blue and methyl orange) that the desorbed amount is about 10% after 6 h of desorption.

CONCLUSION

The present study revealed the feasibility of date pits as an efficient raw precursor for the preparation of activated carbon. Chemical chloride zinc activation showed good development of pore structures, with the surface area, micropore surface area and total pore volume of 1,380 m^2/g, 1,110 m^2/g and 0.91 cm^3/g, respectively. Activated carbon prepared from date pits exhibited amphoteric behavior, indicating its suitability for removal of both anionic (methylene blue) and cationic dyes (methyl orange). Adsorption behavior is described by a monolayer Langmuir type isotherm. Kinetic data follows a pseudo-second-order kinetic model. The maximum adsorption capacities are Q_o=455 and 434 mg·g^{-1} for MB and Mo, respectively, which are comparable with the values for commercial activated carbon reported in earlier studies.

REFERENCES

1. P. C. Vandevivere, R. Bianchi and W. Verstraete, *J. Chem. Technol. Biotechnol.*, **72**, 289 (1998).
2. H. Zollinger, *Color Chemistry*, 2nd Ed., VCH, New York (1991).
3. J. C. Greene and G. L. Baughman, *Textile Chemist Colourist*, **28**, 23 (1996).
4. D. A. S. Phillips, *J. Soc. Dyers Colourists*, **112**, 183 (1996).
5. T. A. Nguyen and R.-S. Juang, *Chem. Eng. J.*, **219**, 109 (2013).
6. A. Bozdogan and H. Goknil, *MU. Fen. Billimeri Dergisi. Sayi.*, **4**, 83 (1987).
7. G. R. Brower and G. D. Reed, *Economical pre-treatment for colour removal from textile dye wastes*, In: Proc. 41st Ind waste conference, Purdue University, West Lafayette, Indiana, 612 (1985).
8. K. Majewska-Nowak, *Desalination*, **71**, 127 (1989).
9. Z. Ding, C. W. Min and W. Q. Hui, *Water Sci. Technol.*, **19**, 39 (1987).
10. J. R. Easton, *The dye maker's view*, In: Cooper, P., *Colour in dye house effluent*, Soc dyers and colorists, Oxford, Alden Press, 6 (1995).
11. J. W. Hassler, Purification with Activated Carbon, 2nd Ed., Chem. Publ. Co., Inc., New York, 171 (1963).
12. G. S. Gupta, G. Prasad and V. N. Singh, *Water Air Soil Pollut.*, **37**, 13 (1988).
13. N. Kannan and M. M. Sundaram, *Dyes Pigm.*, **51**, 25 (2001).
14. N. Kannan, T. Srinivasan and P. Dhandayudhapani, Environ. Media Publishers, 291. Karad, India (1998).
15. S. J. T. Pollard, G. D. Fowler, C. J. Sollars and R. Perry, *Sci. Total Environ.*, **116**, 31 (1992).
16. G. Annadurai and M. R. V. Krishnan, *Indian J. Environ. Protec.*, **16**, 444 (1996).
17. N. Deo and M. Ali, *Indian J. Environ. Protect.*, **17**, 328 (1997).
18. G. McKay, M. S. Otterburn and J. A. Aja, *Water Air Soil Pollut.*, **24**, 307 (1985).
19. M. Danish, R. Hashim, M. N. Mohamad Ibrahim and O. Sulaiman, *Biomass Bioenergy*, **61**, 167 (2014).
20. A. L. Cazetta, O. P. Junior, A. M. M. Vargas, A. P. da Silva, X. Zou, T. Asefa and V. C. Almeida, *J. Anal. Appl. Pyrol.*, **101**, 53 (2013).
21. T. M. Alslaibi, I. Abustan, M. A. Ahmad and A. Abu Foul, *J. Environ. Chem. Eng.*, **1**, 589 (2013).
22. S. S. Ashour, *J. Saudi Chem. Soc.*, **14**, 47 (2010).
23. F. Banat, S. Al-Asheh and L. Al-Makhadmeh, *Chem. Eng. Technol.*, **27**, 80 (2004).
24. A. F. Hassan, W. I. Mortada and M. M. Hassanien, *Inter. J. Modern Chem.*, **5**, 101 (2013).
25. M. Asadullah, I. Jahan, M. B. Ahmed, P. Adawiyah, N. H. Malek and M. S. Rahman, *J. Ind. Eng. Chem.*, **20**, 887 (2014).
26. R. Messaoudi, S. Abbeddou, A. Mansouri, A. C. Calokerinos and P. Kefalas, *Int. J. Food Prop.*, **16**, 1037 (2013).
27. K. S. W. Sing, D. H. Everett, R. A. W. Haul, L. Moscou, R. A. Pierotti, J. Rouquerol and T. Sieminiewska, *Pure Appl. Chem.*, **57**, 603 (1985).
28. H. P. Boehm, Chemical Identification of Surface Groups, In: Eley, D. D., Pines, H., Weisz, P. B. (Ed.), *Advances in Catalysis 16*, Academic Press, New York, 179 (1966).
29. H. P. Boehm, *Carbon*, **32**, 759 (1944).
30. E. Papier, S. Li and J. B. Donnet, *Carbon*, **25**, 243 (1987).
31. S. K. Milongic, V. Antonucci, M. Minutoli and N. Giordano, *Carbon*, **27**, 337 (1975).
32. N. Kannan, *Indian J. Environ. Protect.*, **11**, 514 (1991).
33. A. M. Cunliffe and P. T. Williams, *Environ. Technol.*, **19**, 1177 (1998).
34. H. M. Al-Saidi, *J. Saudi Chem. Soc.*, DOI:10.1016/j.jscs.2013.06.002.
35. S. M. Yakout and G. Sharaf El-Deen, *Arabian J. Chem.*, DOI:10.1016/j.arabjc.2011.12.002.
36. V. Gomez-Serrano, J. Pastor-Viilegas, A. Perez-Florindo, C. Duran-Valle and C. Valenzueia-Calahorro, *J. Anal. Appl. Pyrol.*, **36**, 71 (1996).
37. M. A. Al-Ghouti, J. Li, Y. Yousef Salamh, N. Al-Laqtah, G. Walker and M. N. M. Ahmad, *J. Hazard. Mater.*, **176**, 510 (2010).
38. H. P. Boehm, Chemical Identification of Surface Groups, In: Eley, D. D., Pines, H., Weisz, P. B. (Ed.), *Advances in Catalysis 16*, Academic Press, New York, 179 (1966).
39. A. A. El-Hendawy, *J. Anal. Appl. Pyrol.*, **75**, 159 (2006).
40. L. Huang, Y. Sun, W. Wang, Q. Yue and T. Yang, *Chem. Eng. J.*, **171**, 1446 (2011).
41. L. R. Radovic, C. Moreno-Castilla and J. Rivera-Utrilla, *Carbon materials as adsorbents in aqueous solutions*, In: Radovic, L. R., Ed., *Chemistry and physics of carbon*, Marcel Dekker, New York, **27**, 227 (2001).
42. M. F. R. Pereira, S. F. Soares, J. J. M. Órfão and J. L. Figueiredo, *Carbon*, **41**, 811 (2003).
43. P. C. C. Faria, J. J. M. Órfão and M. F. R. Pereira, *Water Res.*, **38**, 2043 (2004).
44. G. Newcombe and M. Drikas, *Carbon*, **35**, 1239 (1997).
45. W. J. Weber Jr., *Physico-chemical processes for water quality control*, Wiley Interscience, New York, 207 (1972).
46. W. J. Weber and J. C. Morris, In: Eckenfelder, W. W., Ed., *Advances in water pollution research*, Oxford, Pergamon Press (1964).
47. K. R. Hall, L. C. Eagleton, A. Acrivos and T. Vemeulen, *Ind. Eng. Chem. Fund.*, **5**, 212 (1966).
48. A. S. Ozcan and A. Ozcan, *J. Colloid Interface Sci.*, **276**, 39 (2004).
49. S. Langergren and B. K. Svenska, *Veternskapsakad Handlingar*, **24**, 1 (1898).
50. Y. S. Ho and G. McKay, *Chem. Eng. J.*, **70**, 115 (1998).
51. P. K. Malik, *J. Hazard. Mater. B.*, **113**, 81 (2004).
52. C. Namasivayam and D. Kavitha, *Dyes Pigm.*, **54**, 47 (2002).
53. M. S. El-Guendi, *Adsorpt. Sci. Technol.*, **8**, 217 (1991).
54. W. T. Tsai, C. Y. Chang, M. C. Lin, S. F. Chien, H. F. Sun and M. F. Hsieh, *Chemosphere*, **45**, 51 (2001).
55. T. W. Weber and R. K. Chakkravorti, *AIChE J.*, **20**, 228 (1974).
56. F. Haghseresht and G. Lu, *Energy Fuels*, **12**, 1100 (1998).
57. K. Fytianos, E. Voudrias and E. Kokkalis, *Chemosphere*, **40**, 3 (2000).
58. A. W. Adamson, *Physical Chemistry of Surfaces*, 5th Ed. New York, Wiley (1990).
59. S. Chen, J. Zhang, C. Zhang, Q. Yue, T. Li and C. Li, *Desalination*, **252**, 149 (2010).
60. Y. Yao, B. He, F. Xu and X. Chen, *Chem. Eng. J.*, **170**, 82 (2011).
61. K. Mahmoudi, N. Hamdi, A. Kriaa and E. Srasra, *Russ. J. Phys. Chem. A*, **86**, 1294 (2012).
62. T. K. Saha, N. C. Bhoumik, S. Karmaker, M. G. Ahmed, H. Ichikawa

and Y. Fukumori, *J. Water Res. Prot.*, **2**, 898 (2010).
63. N. Zhe-Ming, X. Sheng-Jie, W. Li-Geng, X. Fang-Fang and P. Guo-Xiang, *J. Colloid Interface Sci.*, **316**, 284 (2007).
64. W. S. Tan and C. Liang, *Carbon*, **47**, 1880 (2009).
65. H. Deng, L. Yang, G. Tao and J. Dai, *J. Hazard. Mater.*, **166**, 1514 (2009).
66. E. Dermirbas, M. Kobya and M. T. Sulak, *Bioresour. Technol.*, **99**, 5368 (2008).